

Paper ID code: 32007

Promising Composite Heat Sink Material for the Divertor of future Fusion Reactors

*A. Brendel, C. Popescu, T. Köck, H. Bolt

*Max-Planck-Institut für Plasmaphysik, EURATOM Association, Boltzmannstraße 2,
D-85748 Garching, Germany*

*Corresponding author: Dr. Annegret Brendel

Phone: +49 89 32 99-25 44

Fax: +49 89 32 99-12 12

Annegret.Brendel@ipp.mpg.de

Novel Composite Heat Sink Material for the Divertor of future Fusion Reactors

*A. Brendel, T. Köck, H. Bolt

Max-Planck-Institut für Plasmaphysik, EURATOM Association, Boltzmannstraße 2,
D-85748 Garching, Germany

Abstract

We investigate SiC fibre reinforced copper as an additional layer at the highly loaded zone between plasma facing material (W) and heat sink (CuCrZr) for a fusion reactor divertor.

Copper has a high thermal conductivity of $380 \text{ Wm}^{-1}\text{K}^{-1}$ but a very low strength and creep resistance at 550°C . Therefore copper is reinforced with SiC long fibres (SCS6, Specialty Materials) having excellent high temperature strength.

The fibres were galvanically coated with an $80\text{-}\mu\text{m}$ -thick copper layer as matrix. Hot isostatic pressing at 650°C was applied to form the composite material. The interfacial shear strength calculated from push-out tests was $\sim 6 \text{ MPa}$.

Adding a 100-nm -thin titanium interlayer deposited by magnetron sputtering led to a higher adhesion of the SiC fibres in the copper matrix. Titanium reacted with the carbon surface of the fibre to TiC and formed with copper the alloy Cu_4Ti during heat treatment and increased the interfacial shear strength to 70 MPa .

Keywords: C1000 Copper, C0900 Composite Materials, D0500 Divertor Materials

1. Introduction

In the flat tile concept [1] for a fusion reactor divertor, the component consists of two parts: (i) the direct plasma facing material (PFM) made of carbon or tungsten, and (ii) the heat sink consisting of a copper-rich CuCrZr alloy with cooling tubes [2], [3] which have to transport the heat to the energy conversion and cooling system. This CuCrZr alloy allows an operating temperature of up to 350°C at the interface between the PFM and CuCrZr. Therefore the temperature of the coolant would be limited to 100°C. However, for efficient heat transport within a steam generating cycle of future energy producing reactors (such as DEMO) the coolant temperature should be increased to 300-400°C. In this case the operation temperature of the heat sink is calculated to increase up to 550°C at the interface with the PFM. [4]. The resulting temperature gradient and the thermal expansion mismatch of the divertor parts cause high strain levels at the interface between plasma facing material and heat sink [5]. This zone could be strengthened by insertion of a new material as a third part of the divertor: a composite material consisting of a copper matrix for high thermal conductivity reinforced with SiC long fibres for high strength [6]. The interface between the fibres and the matrix plays a key role for the macroscopic properties [7], [8]. The main purpose of this work is the development of a Cu/SiC composite material with improved interlayer properties. A nanoscopic design feature is the sputtered titanium interlayer as a coupling agent at the interface between fibre and matrix [9], [10]. An adequate thermal treatment initiated a chemical reaction between the titanium and the carbon coating of the fibres. The mechanical characterisation of the composite was performed using push-out tests.

2. Experimental

2.1 Materials and processing

For the long fibre reinforcement of the copper matrix, silicon carbide fibres (SCS6, Specialty Materials) were used. The type of fibre under investigation with 140 μm diameter was originally developed for titanium matrix composites. The fibre consists of a carbon monofilament (30 μm in diameter), two layers of SiC (15 μm of fine-grained β -SiC and 35 μm of coarse-grained β -SiC) and an outer carbon-rich double layer (overall thickness \approx 3 μm), which is bonded to the SiC via a 0.5 μm thick pure amorphous carbon layer. The outer carbon layer is to compensate for surface defects and thus to improve the fibre strength. The fibre structure is shown schematically in Fig. 1 [11].

An approximately 100 nm thick titanium bond layer was deposited on the fibres by magnetron sputtering. Titanium should lead to an improvement of the bond strength between fibre and matrix, due to its reaction with the outer carbon containing layer of the fibre to TiC at temperatures above 350°C [12]. In order to minimize the solution of Ti in the copper matrix, which leads to a reduction of the thermal conductivity, the layer was kept very thin. For matrix deposition the precoated fibres were electroplated with a thick copper layer, using 8 hours at room temperature in a CuSO_4 bath. The thickness of the copper layer defines the fibre volume content of the composite. For a fibre volume content of 20 % the fibres were coated with an 80 μm thick copper layer.

Former works showed that heat treatment at 550°C for 2 hours led to formation of TiC at the interface between fibre and matrix [13]. A very slow heating rate of 0.5 Kmin^{-1} was applied to avoid pore formation by outgassing of hydrogen and oxygen, which both are normally contained in a galvanic layer. The pores, formed as a result of a chemical reaction between hydrogen and oxygen to produce water, would damage the microstructure and decrease the mechanical strength (referred to as pickle brittleness).

To form the composite material, coated and heat-treated single fibres were unidirectional packed in a copper capsule (diameter 10 mm, length 70 mm) as densely as possible. Subsequently the capsule was sealed by welding in vacuum prior to compacting the composite by hot-isostatic pressing at 650°C with a pressure of 100 MPa for 30 minutes. The fibre reinforced zone has a diameter of 3.5 mm.

2.2 Mechanical characterisation of the interface

Push-out tests were performed for the mechanical characterisation of the interface between the fibre and matrix. The fibre length varied between 0.4 and 3 mm. Single fibres were pushed out of the matrix with a flat-ended punch of 100 µm diameter by means of a specially designed universal test machine. The load was measured with a load cell during testing while the indenter was moved in displacement control mode following a ramp of 1 µms⁻¹. Both the resulting load and the indenter displacement were recorded continuously. The load vs. displacement curve (Fig. 2) is different for composite samples with or without the TiC interlayer. For a composite specimen without a TiC interlayer the curve shows an elastic increase of the load until the first local maximum, which indicates the beginning of debonding. This point is called the debonding load - P_d [14]. In the further curve progression, the debonding is superposed with friction. At the absolute maximum load - P_{max} [14], the fibre breaks free of the matrix. The resulting force, which depends on the level of push-out friction, decreases during the final phase of the experiment. In the case of a composite with a TiC interlayer the curve shows the first maximum as the absolute maximum, which is called P_d . After debonding the load jumps to a low level and rises again to a second, intermediate maximum P_{max} (definition see [14]) characterising the push-out friction.

Two interface parameters (i) interfacial shear strength τ_d (maximum shear stress encountered at the fibre/matrix interface just prior to P_d) and (ii) interfacial friction stress τ_f (causes the reactive force during fibre slip opposite to the moving direction [14]) were calculated by means of shear lag based models. These models describe the transfer of tensile stress from the matrix to the fibre, as originally proposed in [15]. For the estimation of failure relevant parameters in fibre reinforced composites, like stress distribution and stress concentration, the shear lag analysis is a common model. It is characterised by the simplified consideration of three-dimensional fibres as one-dimensional entities. The debonding load P_d in pull-out tests can be related to τ_d by Eq.1 using a shear lag analysis [16], [17], which also can be extended to *push*-out tests [18].

$$P_d = \frac{\tau_d \cdot 2\pi R}{\alpha} \cdot \tanh(\alpha \cdot L) \quad (1)$$

(R fibre radius; L specimen thickness, equivalent to the fibre length; α shear lag parameter, dependent on the relative elastic properties of fibre and matrix and their geometric configuration)

An iterative regression of Eq.1 can be used for a series of push-out tests of composite specimens with different sample thickness, i.e. different fibre lengths L, for determination of τ_d .

In [19] the interfacial friction stress in ceramic matrix composites was estimated for the case of frictionally bonded fibre matrix interfaces, but is also valid for chemically bonded interfaces.

Two intrinsic parameters, a coefficient of friction μ , and a radial residual stress σ_0 , caused by the different coefficients of thermal expansion of the fibre and the matrix characterise the frictional bonding of the interface. The following linear friction law is assumed:

$$\tau_f = \mu \cdot \sigma_0 \quad (2)$$

The maximum load P_{\max} of a series of push-out tests on composite specimens with varying thickness, i.e. different embedded lengths of fibre, provides a basis for the experimental determination of the interfacial parameters μ and σ_0 by means of a nonlinear regression of Eq. 3.

$$P_{\max} = \frac{\pi R^2 \sigma_0}{k} \left[\exp\left(\frac{2\mu k}{R} \cdot L\right) - 1 \right] \quad \text{with} \quad k = \frac{v_f E_m}{E_f (1 + v_m)} \quad (3)$$

(E, v Young's modulus and Poisson's ratio; the indices f, m denote fibre and matrix, resp.)

3. Results and Discussion

The interfacial shear strength τ_d and the interfacial friction stress τ_f describe the mechanical interface properties. Both values were calculated from approximately 20 pushed fibres of each sample. The mean values of the debonding load P_d vs. the sample thickness were used for the determination of the interfacial shear strength τ_d (Fig. 3). The circle symbols correspond to the results obtained from a composite without a TiC interlayer and triangles to a composite with TiC interlayer. The P_d function (Eq. 1) was fitted to the data points with τ_d and α as fit parameters (shown by curves). The interfacial shear strength was calculated to be 6 MPa for samples without a titanium carbide interlayer and 70 MPa for samples with the titanium carbide interlayer.

Fig. 4 shows the mean values of the maximum load P_{\max} vs. the sample thickness for the calculation of τ_f . The P_{\max} function (Eq. 3) was fitted to the data points with σ_0 and μ as fit parameters (curves). The calculated friction stress τ_f was 4 MPa for composites without, and 54 MPa for composites with titanium carbide interlayer.

The cause of the weak bonding between SiC fibre and copper matrix without a TiC interlayer (τ_d and τ_f are less than 10 MPa) is the 3 μm carbon-rich double layer at the surface of the SCS6-SiC fibre. The outer carbon-rich double layer prevents a reaction with the copper matrix. Fig. 5 shows a SEM image of such a slipped fibre. No matrix material adheres to the fibre surface and no deformation of the copper matrix can be observed. The carbon layer acts as a lubricant, so that the fibres could be easily pushed out under almost frictionless sliding. With a titanium carbide interlayer as a coupling agent the values for interfacial shear strength and interfacial friction stress are at least tenfold higher compared to the samples without a titanium carbide interlayer, indicating a high bonding strength between the SiC fibre and copper matrix. Titanium reacted with the carbon-rich layer of the fibre surface, forming TiC (former work, detection by EELS [13]), and with the copper matrix to form Cu_4Ti (detection by XRD, former work on planar carbon substrates with similar layer structure [20]) during the heat treatment. Thus, titanium acted both chemically and mechanically to improve the bonding process.

The SEM image (Fig. 6) of a pushed out fibre of a composite specimen with a TiC interlayer shows a completely different behaviour compared to the TiC-free case. In the centre of the picture the carbon-rich double layer is still bonded via the thin TiC interlayer to the copper matrix after push-out test in contrast to the case without the TiC layer (Fig. 5). In this case the amorphous carbon layer between SiC and the outer carbon-rich double layer of the fibre failed first. The fibre core region itself moves longitudinally during the push-out tests by shear and displacement processes.

4. Conclusions

A thin TiC interlayer leads to improved bonding between a SiC fibre and the copper matrix. Titanium was deposited by magnetron sputtering with a thickness of 100-200 nm at the fibre.

During the heat treatment at 550°C TiC was formed with the outer carbon-rich double layer of the fibre surface. This carbide formation at the fibre/matrix interface caused micromechanical effects, which lead to an increase of the interfacial shear strength and interfacial friction stress by one order of magnitude in relation to composites without a TiC interlayer. A steady growth of Cu₄Ti is not expected since the amount of Ti is limited. However, the Ti interlayer should be as thin as possible to prevent the copper matrix from degradation of thermal conductivity.

Acknowledgement

The authors would like to thank H. Schurmann (DLR, Cologne) for performing the hot-isostatic pressing.

A part of this work has been performed within the framework of the Integrated European Project „ExtreMat“ (contract NMP-CT-2004-500253) with financial support by the European Community. It only reflects the view of the authors and the European Community is not liable for any use of the information contained therein.

References

- [1] EFDA, A Conceptual Study of Commercial Fusion Power Plants, Final Report of the European Fusion Power Plant Conceptual Study (PPCS), EFDA-RP-RE-5.0, September 15th, 2004.
- [2] G. Kalinin, W. Gauster, R. Matera, A.A.F. Tavassoli, A. Rowcliffe, S. Fabritsiev, H. Kawamura, Journal of Nuclear Materials, 233-237 (1996) 9-16.
- [3] A. A. F. Tavassoli, Journal of Nuclear Materials 258-263 (1998) 85-96.
- [4] A. S. Kukushkin, H.D. Pacher, G. Federici, G. Janeschitz, A. Loarte, G. W. Pacher, Fusion Engineering and Design 65 (2003) 355-366.

- [5] J. H. You, H. Bolt, Journal of Nuclear Materials 299 (2001) 1-8.
- [6] J. H. You, H. Bolt, Journal of Nuclear Materials 305 (2002) 14-20.
- [7] J. Woltersdorf, E. Pippel, A. Hähnel, Zeitschr. f. angew. Math. u. Mechan. (Wiley-VCH) 78, Suppl.1, S81-S84 (1998).
- [8] J. Woltersdorf, Nova Acta Leopoldina NF 317, 253-282 (2000).
- [9] Neubauer E., Eisenmenger-Sittner C., Bangert H., Korb, G.; Vacuum. 71(1-2):293-298, 2003 May 9.
- [10] Matsunaga K, Ikuhara Y, Jung YC, Kim SS, Lee SK; Journal of the Ceramic Society of Japan 113 (1320) 540-542 Aug 2005.
- [11] P. R. Smith, M. L. Gambone, D. S. Williams, D. I. Garner, Journal of Materials Science 33 (1998) 5855-5872.
- [12] S. Miller, Dissertation, Universität Bayreuth, 1997.
- [13] A. Brendel, J. Woltersdorf, E. Pippel, H. Bolt, Materials Chemistry and Physics 91 (2005) 116–123.
- [14] G. Rausch, B. Meier, G. Grathwohl, Journal of European Ceramic Society 10 (1992) 229-235.
- [15] H. L. Cox, British Journal of Applied Physics (1952) 72-79.
- [16] L.B. Greszczuk, Interfaces in Composites, ASTM Special Technical Publication 452, American Society of Testing and Materials, Philadelphia (1969) 42-58.
- [17] P. Lawrence, Journal of Material Science 7 (1970) 1-6.
- [18] J. D. Bright, D. K. Shetty, C. W. Griffin, S. Y. Limaye, Journal of American Ceramic Society 72 (1998) 1891-1898.
- [19] D. K. Shetty, Journal of American Ceramic Society 71 (1988) C-107-C-109.
- [20] A. Brendel C. Popescu, H. Schurmann, H. Bolt, Surface & Coatings Technology, Special issue: Plasma Surface Engineering (PSE 2004), Vol 200/1-4 pp 161-164.

Figure captions

Fig. 1: Structure of the SiC fibre (SCS6, Specialty Materials)

Fig. 2: Push out test: schematic load vs. displacement diagram of samples with and without TiC interlayer [14]

Fig. 3: Push-out test: debonding load vs. sample thickness

Fig. 4: Push-out test: maximum load vs. sample thickness

Fig. 5: SEM: pushed fibre of a composite without titanium interlayer. Only the outermost carbon layer of the fibre is shown.

Fig. 6: SEM: pushed fibre of a composite with titanium carbide interlayer. In this case two components of the fibre are shown-the outermost carbon-rich double layer and the coarse grained β SiC layer.

Figures

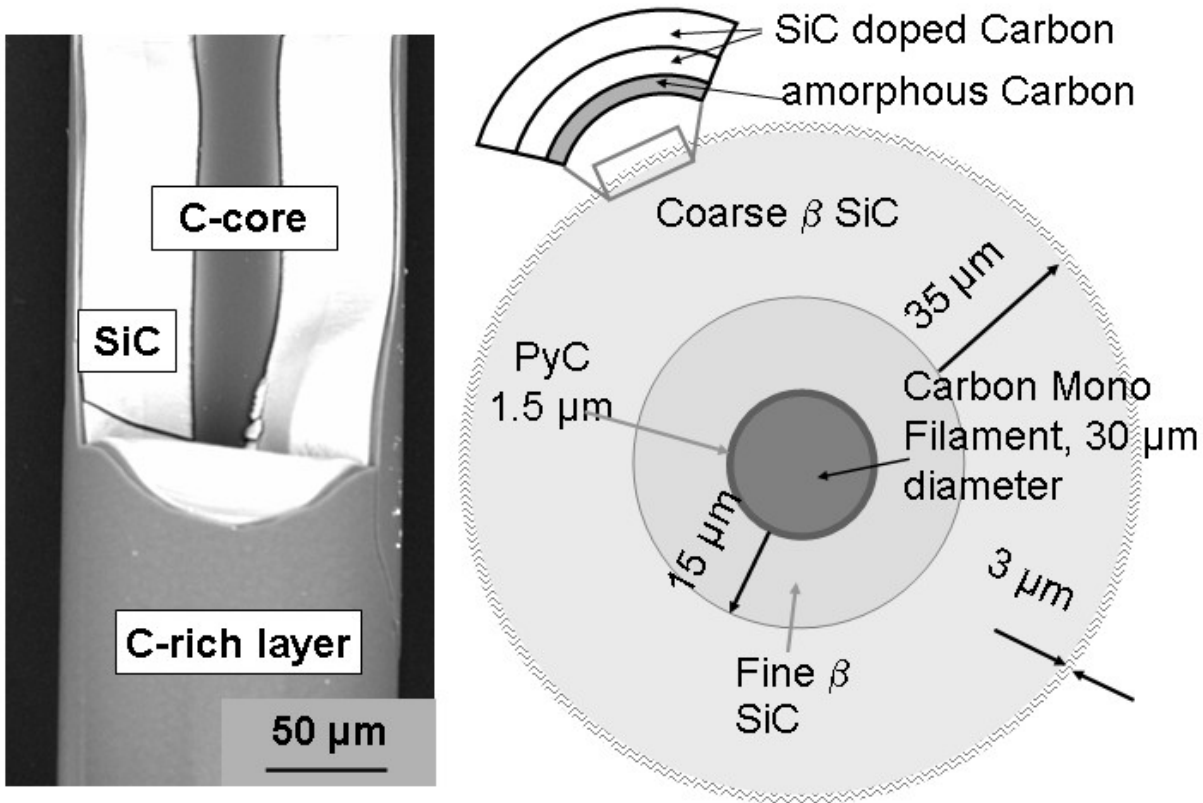


Fig. 1: Structure of the SiC fibre (SCS6, made by Specialty Materials)

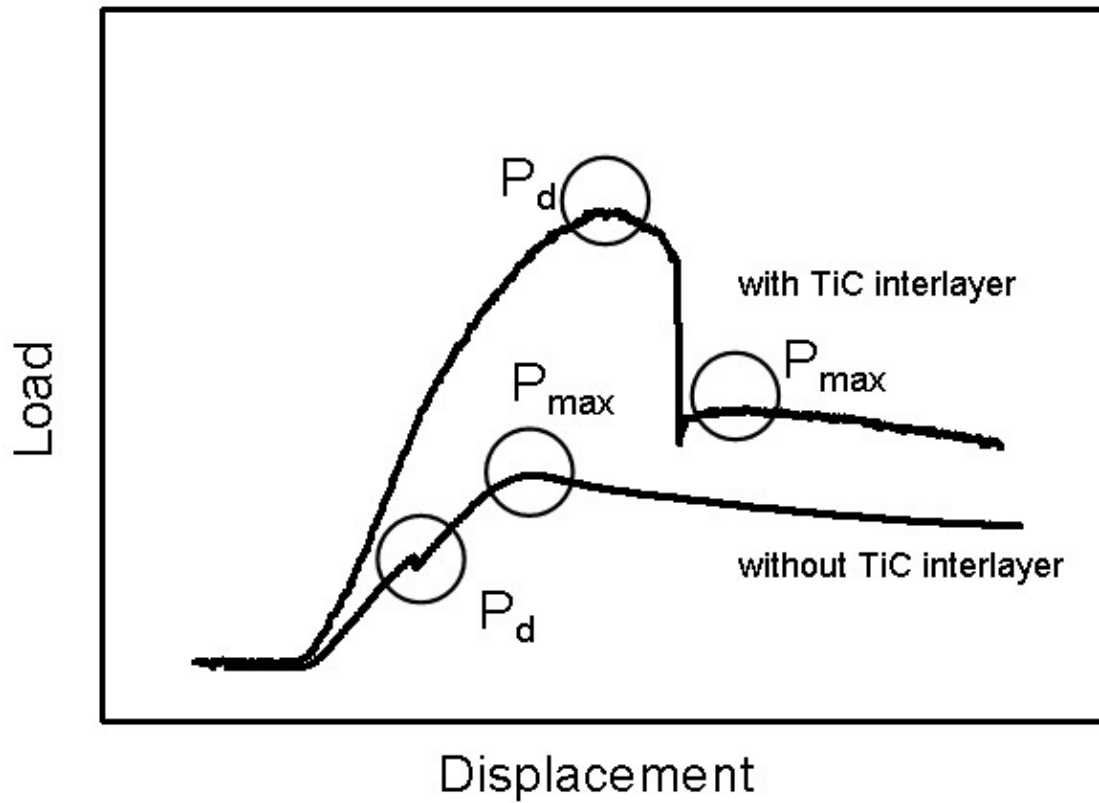


Fig. 2: Push out test: schematic load vs. displacement diagram of samples with and without TiC interlayer [14]

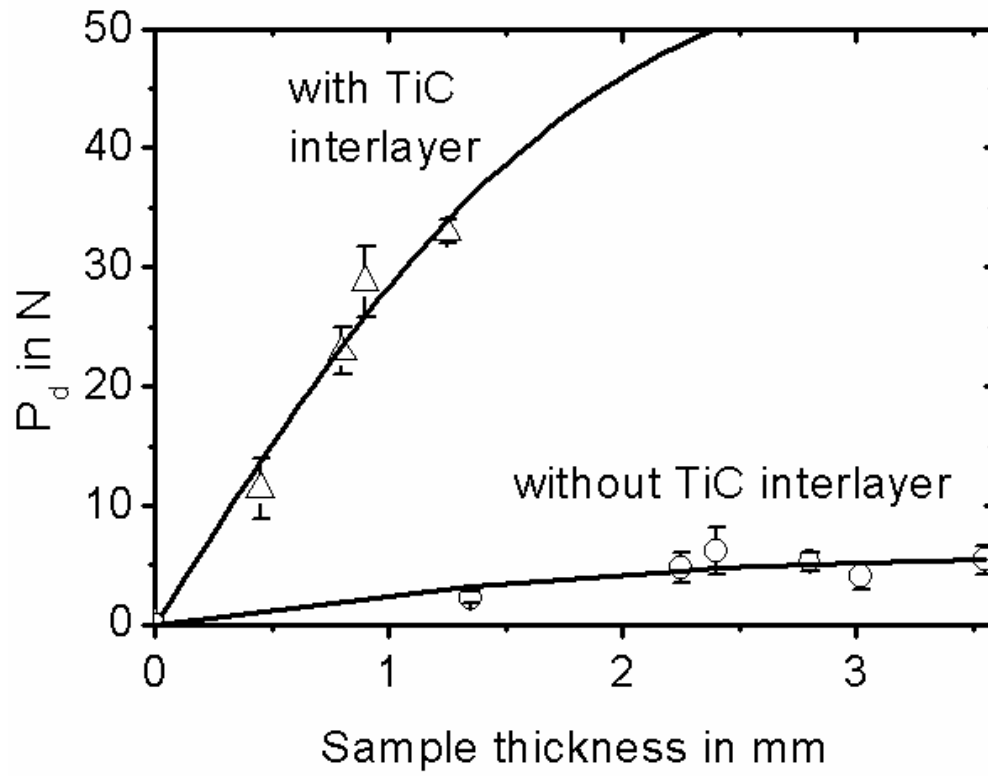


Fig. 3: Push-out test: debonding load vs. sample thickness

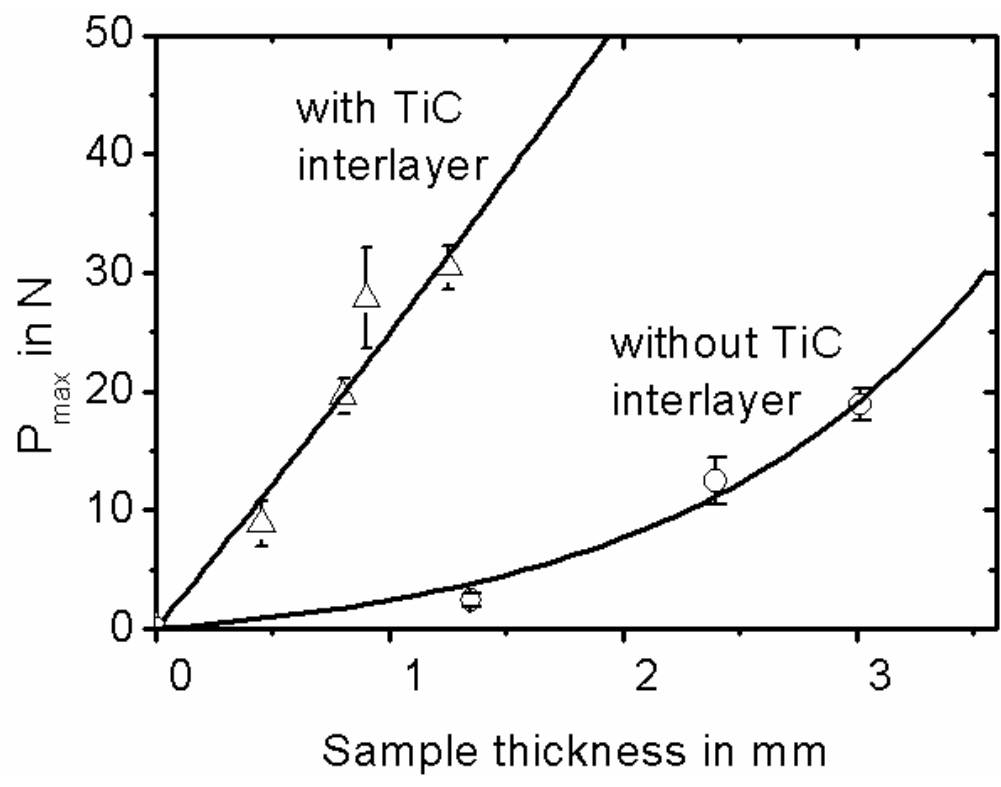


Fig. 4: Push-out test: maximum load vs. sample thickness

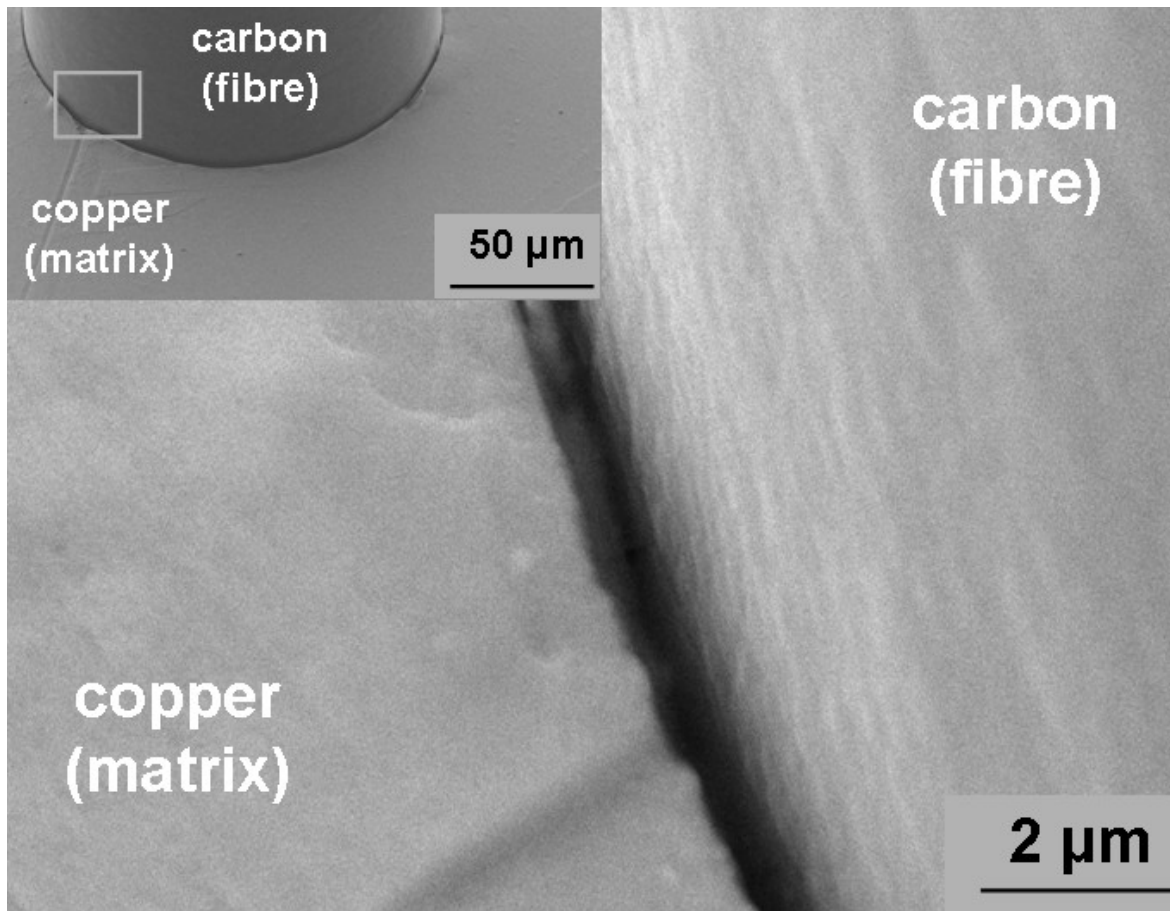


Fig. 5: SEM: pushed fibre of a composite without titanium interlayer. Only the outermost carbon layer of the fibre is shown.

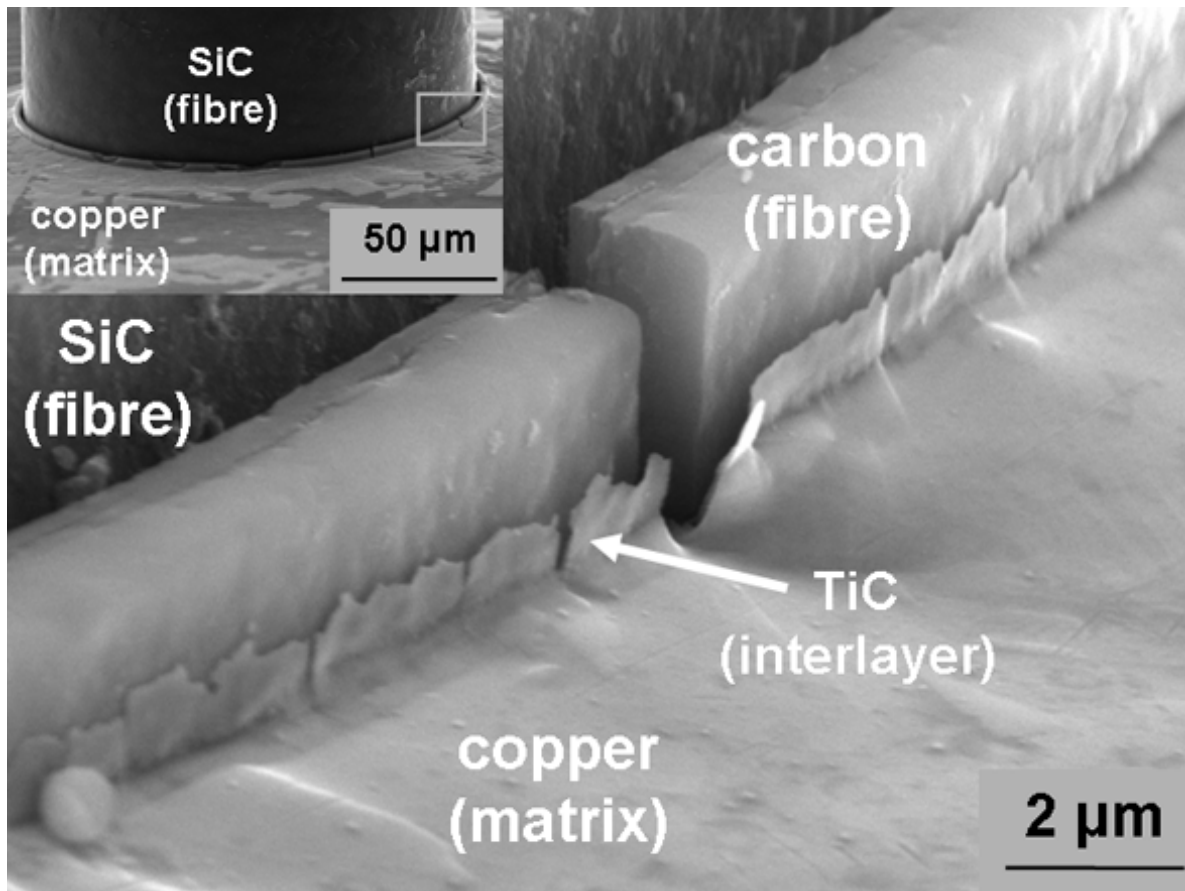


Fig. 6: SEM: pushed fibre of a composite with titanium carbide interlayer. In this case two components of the fibre are shown-the outermost carbon-rich double layer and the coarse grained β SiC layer.